Vibrational spectra of a Ca-Nb-Ga garnet (CNGG) single crystal studied by Raman and infrared reflectivity spectroscopy

1998 J. Phys.: Condens. Matter 10 6865

(http://iopscience.iop.org/0953-8984/10/31/005)

J. Phys.: Condens. Matter **10** (1998) 6865–6873. Printed in the UK PII: S0953-8984(98)91456-4

Vibrational spectra of a Ca–Nb–Ga garnet (CNGG) single crystal studied by Raman and infrared reflectivity spectroscopy

K Shimamura†, P Becker‡, B Wyncke§, F Bréhat§, T Fukuda† and C Carabatos-Nédelec‡‖

† Institute for Material Research, Tohoku University, 2-1-1 Katahira, Aoba-ku, Sendai 980, Japan

‡ Centre Lorrain d'Optique et Electronique des Solides, Université de Metz et Supélec, Technopôle de Metz 2000, 2 Rue Edouard Belin, 57078 Metz Cédex 3, France

§ Equipe Infrarouge Lointain, Université de Nancy 1, BP 239, 54506 Vandoeuvre lès Nancy Cédex, France

Received 9 February 1998

Abstract. Calcium niobium gallium garnet (CNGG), a new non-linear optical material, is studied by Raman and infrared reflectivity spectroscopy at low and at room temperature for various scattering configurations. No structural phase transition is observed in the temperature range of the experiments. The phonons are classified within their symmetry species in the $I2_13 = T^5$ space group assumption; their dynamical parameters such as wavenumber, damping and oscillator strength are obtained on the basis of the infrared reflectivity spectra analysis. The comparison of the infrared and Raman activity of the phonon modes is in favour of the aforementioned space group; however, Pockels electrooptic coefficient room temperature measurements did not allow us to confirm this space group.

1. Introduction

Calcium niobium gallium garnet (CNGG) is a new non-linear optical material and solid-state laser host, and can be activated over a wide wavelength region by doping with rare earth elements [1]. Its crystal growth [1], structure [2] and rare earth element doping [3] have been studied by Shimamura *et al*. Although some visible light absorption [1] and dielectric [3] data have been published, spectroscopic experiments are scarce; the Raman spectrum of CNGG is unknown, as well as its infrared one.

The aim of the present paper is to study and analyse as completely as possible the polarized phonon spectra of a CNGG single crystal in the low wavenumber region 10–1000 cm^{-1}, at room temperature and at low temperature, by using and comparing Raman and infrared reflectivity spectroscopy.

2. Structure and symmetry

Ono *et al* [3] have studied the composition and crystal structure of CNGG. They concluded that the compound is highly non-stoichiometric with the formula $Ca_{2.9}Nb_{1.6}Ga_{3.3}O_{12}$.

‖ Author to whom correspondence should be addressed. E-mail address: ccarabat@iut.univ-metz.fr.

0953-8984/98/316865+09$19.50

Besides a subsisting possibility that the space group of CNGG is the centrosymmetric $Ia3d = O_h^{10}$ (No 230), they assigned the non-centrosymmetric space group $I2_13 = T^5$ (No 199). In this latter assignment, two calcium ions occupy sites of type 12b (Wyckoff notation) with general position $(x, \frac{1}{4}, 0)$ and one calcium ion occupies an 8a type of site $(\frac{1}{4}, \frac{1}{4}, \frac{1}{4})$ with a probability of 0.1, whereas a niobium ion occupies the same site with a probability of $\sim$0.9. A second niobium ion occupies another 8a type of site at $(0, 0, 0)$ with a probability of $\sim$0.7, whereas a gallium ion occupies the same site with a probability of $\sim$0.3. Two other gallium ions occupy sites of type 12b and general position $(x, 0, \frac{1}{4})$. Figure 1 illustrates the elementary cell of CNGG for this space group; it contains eight formula units. The lattice constant is $a = 12.5472$ Å [3]. For the sake of simplicity, we model the structure by the formula $Ca_3^{(1,2)}XYGa_3^{(1,2)}O_{12}^{(1,4)}$ where $X = Ca_{0.099}^{(3)}Nb_{0.901}^{(1)}$, $Y = Ga_{0.29}^{(3)}Nb_{0.71}^{(2)}$, the upper indices indicating the ion number in table 1 of [3] and the lower indices the probability of occupation. With this molecule model, one has $8 \times 20 = 160$ 'ions' in the elementary cell, implying a dynamical space of dimension 480.

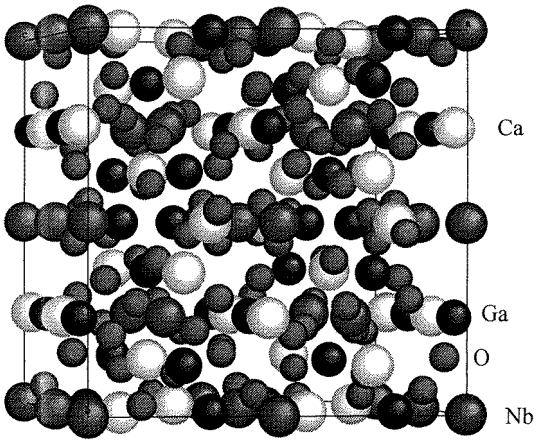

Figure 1. The elementary cell of CNGG in the $I2_13 = T^5$ symmetry case.

At zero wavevector, the irreducible representations of the vibrational modes in the aforementioned $I2_13 = T^5$ space group are the following:

$$\Gamma_{vib} = 40A^R(xx + yy + zz) + 40E^R(xx + yy - 2zz; xx - yy) + 120F^{R,IR}(xy, yz, zx; x, y, z; Rx, Ry, Rz)$$

where the upper indices R or IR indicate Raman or infrared activity and between parentheses are given the polynomial and rotational basis functions (polarization).

The Raman scattering tensors are

$$\tilde{R}_A = \begin{pmatrix} a & 0 & 0 \\ 0 & a & 0 \\ 0 & 0 & a \end{pmatrix} \qquad \tilde{R}_{E_1} = \begin{pmatrix} b + \sqrt{3}c & 0 & 0 \\ 0 & b - \sqrt{3}c & 0 \\ 0 & 0 & 2b \end{pmatrix}$$

$$\tilde{R}_{E_2} = \begin{pmatrix} c - \sqrt{3}b & 0 & 0 \\ 0 & c + \sqrt{3}b & 0 \\ 0 & 0 & -2c \end{pmatrix}$$

and the infrared activity tensors are

$$\tilde{I}_{F_1} = \begin{pmatrix} 0 & 0 & 0 \\ 0 & 0 & d \\ 0 & d & 0 \end{pmatrix} \qquad \tilde{I}_{F_2} = \begin{pmatrix} 0 & 0 & d \\ 0 & 0 & 0 \\ d & 0 & 0 \end{pmatrix} \qquad \tilde{I}_{F_3} = \begin{pmatrix} 0 & d & 0 \\ d & 0 & 0 \\ 0 & 0 & 0 \end{pmatrix}.$$

One thus expects 80 Raman active but infrared inactive modes of species A and E and 117 Raman and infrared active modes of species F in addition to the three acoustic modes of species F.

Taking into account the weights of the ions and the types of bond, it is rather clear that the phonon wavenumbers will lie below $\sim$1000 cm^{-1}, hence the 'mean distance' between two phonon lines is $\sim$25 cm^{-1} for the A and E Raman spectra and $\sim$8 cm^{-1} for the Raman and infrared F spectra, predicting overlaps and coincidences of many lines.

If one decides in favour of the centrosymmetric $Ia3d = O_h^{10}$ space group, things are easier because the phonons are either Raman active or infrared active. We thus hope that the following study will be able to enforce one or the other of the two possibilities.

3. Experimental infrared and Raman results

3.1. Experimental conditions

The single crystal studied was grown by one of the authors (KS) using a conventional RF heating Czochralski–Kyropoulos furnace with platinum or iridium crucible [1]. The sample used for infrared reflectivity measurements was a parallelepiped of size 20 mm $\times$ 12 mm $\times$ 7 mm, with the face (100) polished to optical quality, allowing the study of the F infrared active modes.

The far infrared reflectivity spectra of CNGG were measured at 10 K, 100 K and room temperature, with an angle of incidence of $\sim$10°, from 10 to 600 cm^{-1} for the low temperatures. The spectral range was extended from 600 to 4000 cm^{-1} at 300 K by using a Perkin Elmer grating infrared spectrometer model 457.

The Raman experiments were performed on a CNGG sample cut and oriented in order to exhibit all the (100) type of face which were polished to optical quality. The sample orientation was achieved by using the back-reflected laser beam; the scattered light was collected at 90°. The Raman spectrometer was a Spex double monochromator with a photon counting read-out system using a Peltier effect cooler for the RCA C31034 photomultiplier. The whole system was driven by a Spex Datamate controller and acquisition processor with adequate floppy discs. For the low temperature measurements, the CNGG sample was cooled in an Air-Product Displex cryostat driven by an automatic temperature controller and indicator. The laser beam used was the 5145 Å argon ion line.

3.2. Infrared reflectivity spectra

Figure 2 shows the far infrared reflectivity spectra of CNGG from 20 to 600 cm^{-1} for the low temperatures and from 20 to 1500 cm^{-1} for room temperature.

Below 50 cm^{-1}, for each temperature, we observe a flat reflectivity, the level of which depends upon the temperature. Table 1 indicates the values of this long wavelength reflectivity, as well as the corresponding static dielectric constant; the comparison with the published value for the latter at room temperature is quite favourable.

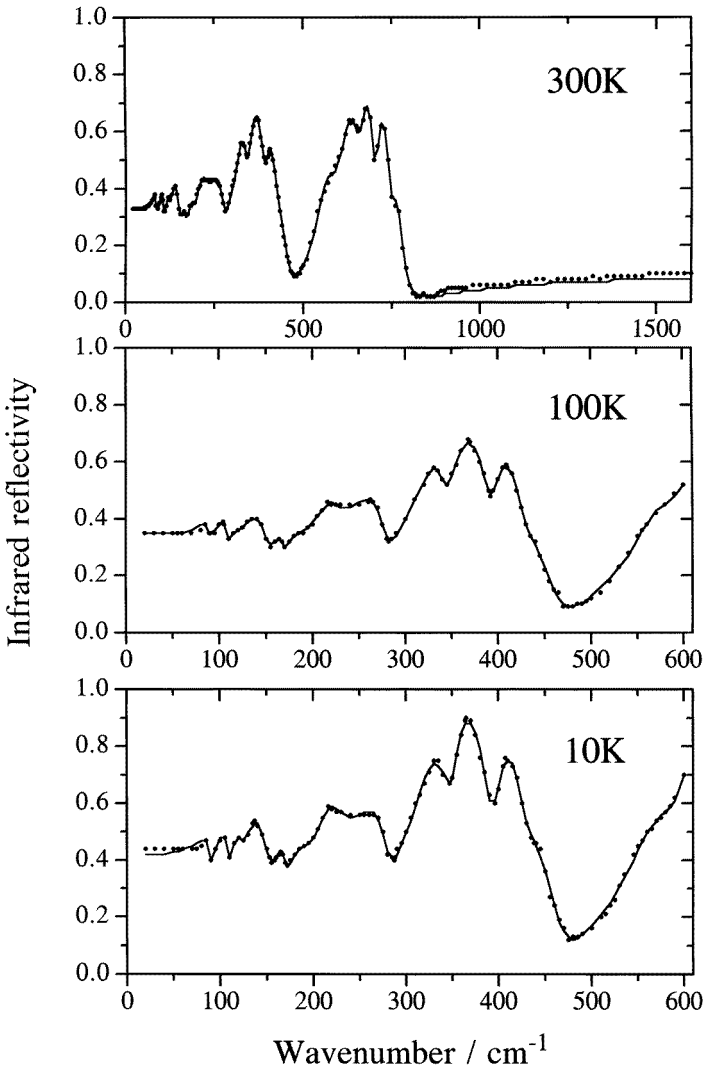

Figure 2. Infrared reflectivity of CNGG at three temperatures: 300, 100 and 10 K.

Table 1. Infrared reflectivities and static dielectric constant of CNGG.

Temperature (K)	IR reflectivity	IR deduced ε_s	Literature ε_s [3]
10	0.42	22	—
100	0.35	15	—
300	0.33	14	16

One observes broad reflectivity peaks, envelopes of narrower neighbouring peaks, in accord with the predicted overlapping due to the large number of peaks in a relatively restricted wavenumber range (cf section 2) and to the normal resolution limitations of the spectrometer.

3.3. Raman scattering

Figure 3 shows the Raman spectra of the CNGG single crystal sample at 10 K in the wavenumber range 10–1000 cm^{-1} for the four polarizations YY, XY, YZ and ZX. We recall that in the case of $I2_13 = T^5$ symmetry, YY belongs to the A and/or E species, exclusively Raman active, and XY, YZ and ZX belong to the F species, both infrared and Raman active. In the case of an $Ia3d = O_h^{10}$ symmetry, YY belongs to the A_{1g} and/or E_g species, exclusively Raman active, whereas the XY, YZ and ZX belong to the *gerade* F_{2g} species, exclusively Raman active as well; in the latter case, the exclusively infrared active modes belong to the *ungerade* F_{1u} species.

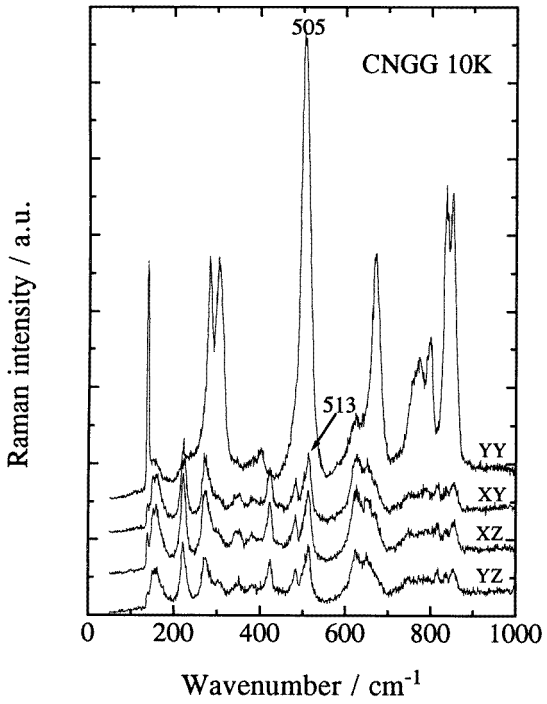

Figure 3. Raman spectra of CNGG at 10 K for four different polarizations.

The spectra exhibit a rather complicated structure with ∼17 peaks and quite spread-out intensities, much stronger in the YY spectrum than in the off-diagonal ones. Again one observes the influence of overlapping and coincidence of the lines.

4. Analysis and discussion

4.1. Analysis of the infrared spectra

The optical mode parameters, wavenumber Ω_j and damping γ_j for each active phonon mode j, were obtained by fitting the factorized form of the dielectric function [4–6]:

$$\varepsilon(\omega) = \varepsilon_\infty \prod_j \frac{\Omega_{jLO}^2 - \omega^2 + i\gamma_{jLO}\omega}{\Omega_{jTO}^2 - \omega^2 + i\gamma_{jTO}\omega} \tag{1}$$

to the experimental reflectivity spectra. At normal incidence, the reflectivity $R(\omega)$ is given by

$$R(\omega) = \left[\frac{\sqrt{\varepsilon(\omega)} - 1}{\sqrt{\varepsilon(\omega)} + 1}\right]^2. \tag{2}$$

In relation (1), Ω_{jTO} and Ω_{jLO} are the transverse (TO) and longitudinal (LO) wavenumbers of mode j respectively, γ_{jTO} and γ_{jLO} the corresponding dampings and ε_∞ the high frequency (optic) dielectric constant.

The initial wavenumber values for the fitting process were deduced from a preliminary Kramers–Kronig analysis of the experimental data. The values of the optical mode parameters obtained in a first step were then improved by a non-linear least squares fit of the reflectivity spectra. Table 2 lists the optical mode parameters obtained by this fit for the three temperatures of experimentation. Figure 2 displays the good agreement between the fit and the experiment.

The oscillator strengths of the modes were calculated from the whole set of TO and LO optical mode wavenumbers of table 2, using the relation

$$S_j = \varepsilon_\infty \left(\frac{\Omega_{jLO}^2}{\Omega_{jTO}^2} - 1\right) \prod_{j \neq k} \frac{\Omega_{kLO}^2 - \Omega_{jTO}^2}{\Omega_{kTO}^2 - \Omega_{jTO}^2}. \tag{3}$$

They are listed in table 2. The static dielectric constants were deduced from the low wavenumber infrared reflectivity (see table 1). The room temperature difference of the static and optic dielectric constants $\varepsilon_0 - \varepsilon_\infty \cong 14 - 4 = 10$ is quite high, thus indicating a rather ionic crystal and a quite large overall oscillator strength. This value is to be compared to the sum of the individual oscillator strengths of table 2, that is to the value of 9,6 for room temperature.

4.2. Analysis of the Raman spectra

As stated above, because of the large number of atoms in the elementary cell, the Raman spectra should contain many bands owing to phonons of longitudinal, transverse or mixed polarization character. The well resolved 10 K spectra show only about 17 peaks of various intensities. This low number is to be compared to the predicted 80 in the A and E species and to the 117 in the F species; the reasons have been explained above (see section 2).

In figure 3 one observes the important difference in scattering intensity between the A+E species (YY polarization) on one hand and the F species (XY, YZ and ZX polarization) on the other hand.

Table 3 lists the wavenumbers (in cm^{-1}) obtained by both infrared reflectivity and Raman scattering with the indication of the intensities. Inspection of table 3 shows that besides some overlaps due to the large number of modes, the principal peaks (underlined values in the table) in the YY diagonal polarization do not correspond to infrared TO, LO or mixed polarization modes. On the contrary, most of the off-diagonal polarization Raman modes exhibit peaks corresponding to TO, LO or mixed polarization infrared modes within reasonable deviations due to the lower accuracy of the infrared wavenumber determinations and to overlaps.

The Raman peaks at 305 and 505 cm^{-1} seem to originate in the Ca–O and Nb–O bonds (respectively), as manifested in the TO phonons of CaO [7] and $KNbO_3$ [8] single crystals (respectively).

At this stage, our measurements are in accord with [2], that is they are in favour of the $I2_13 = T^5$ space group (see above, section 3.2).

Table 2. Dynamical parameters of the infrared reflectivity analysis of CNGG for three temperatures: 300, 100 and 10 K.

j	Ω_{jLO}	γ_{jLO}	Ω_{jTO}	γ_{jTO}	S_j
300 K					
1	85.3	7.1	84.1	7.7	0.46
2	106.2	7.7	104.6	8.1	0.48
3	121.2	7.4	120.5	7.2	0.18
4	149.5	23.1	141.5	19.1	1.43
5	166.1	9.6	165.1	8.6	0.11
6	188.4	16.4	187.2	15.0	0.15
7	216.5	47.5	215.0	28.9	0.26
8	275.9	31.0	263.5	39.3	1.48
9	340.6	25.9	326.2	23.8	1.99
10	392.0	25.2	355.5	24.2	1.53
11	427.7	35.3	398.2	23.0	0.23
12	456.2	55.2	430.4	38.0	0.04
13	567.4	104.5	559.9	39.3	0.19
14	660.8	47.6	617.3	45.4	0.88
15	700.3	26.4	669.8	33.3	0.11
16	750.0	29.8	708.6	23.9	0.06
17	778.1	41.4	756.4	24.2	0.01
100 K					
1	86.2	7.0	85.4	6.8	0.27
2	106.1	6.2	104.9	6.2	0.32
3	120.7	7.3	120.5	7.7	0.03
4	149.9	19.5	143.0	20.9	1.32
5	166.7	8.4	165.6	8.1	0.13
6	188.6	15.5	187.7	15.4	0.13
7	218.7	39.9	216.0	25.3	0.39
8	278.8	23.8	265.5	37.9	1.70
9	343.6	21.7	326.0	32.3	2.53
10	390.8	22.2	353.4	23.1	1.07
11	426.2	29.0	397.9	21.6	0.24
12	459.9	45.6	430.8	38.8	0.07
13	589.8	75.1	562.6	46.5	0.62
14	655.5	30.9	607.2	46.9	0.27
15	690.8	19.9	671.9	37.4	0.05
16	737.0	21.8	713.8	31.9	0.06
17	771.7	19.9	760.5	34.6	0.02
10 K					
1	88.0	5.9	86.7	7.7	0.77
2	107.2	5.4	105.6	6.8	0.81
3	121.3	7.6	120.2	7.8	0.53
4	151.8	23.4	139.5	20.2	3.38
5	167.3	9.9	165.6	8.3	0.25
6	189.2	17.2	187.4	15.7	0.35
7	224.4	50.2	216.1	22.0	1.52
8	280.1	23.8	264.2	38.6	2.47
9	348.2	21.1	319.5	24.7	3.73
10	389.8	21.7	354.1	13.4	0.59
11	425.3	27.5	398.5	21.7	0.31
12	463.7	38.6	429.7	40.3	0.09
13	589.8	75.4	556.1	46.7	0.90
14	657.9	25.6	606.3	35.5	0.34
15	696.2	13.3	668.6	44.3	0.08
16	746.0	14.7	707.7	42.9	0.07
17	783.8	10.0	750.2	49.8	0.01

Table 3. CNGG wavenumbers (cm^{-1}) at 10 K.

	Infrared reflectivity			Raman polarization	
j	Ω_{jTO}	Ω_{jLO}	S_j	YY	XY, YZ, ZX
1	87	88	0.77		
2	106	107	0.81	106sh	
3	120	121	0.53		
				137s	139sh
4	139	152	3.38	154sh	156m
5	166	167	0.25		
6	187	189	0.35		
7	216	224	1.52		222m
				230sh	
8	264	280	2.47		
				284s	
				305s	302sh
9	319	348	3.73	345sh	348w
				375sh	
10	354	390	0.59		383vw
11	398	425	0.31	401w	
12	430	464	0.09		423m
					449sh
					482w
				505vs	
					513m
13	556	590	0.9		
				626w	625m
14	606	658	0.34		654w
15	667	696	0.08	670s	
16	708	746	0.07	758sh	751sh
17	750	784	0.01	774m	
				798m	791w
					815w
				838s	834w
				850s	854w

vs, very strong; s, strong; m, mean; w, weak; vw, very weak; sh, shoulder.

4.3. Electrooptic Pockels coefficient

The conclusion of section 4.2 implies that one can expect the presence of non-vanishing Pockels electrooptic coefficients, whereas in the case of a centrosymmetric $Ia3d = O_h^{10}$ group, all Pockels coefficients vanish by symmetry.

In the case of the $I2_13 = T^5$ group, the Pockels coefficients tensor of rank 3 has the form

$$\begin{pmatrix} 0 & 0 & 0 \\ 0 & 0 & 0 \\ 0 & 0 & 0 \\ r_{41} & 0 & 0 \\ 0 & r_{41} & 0 \\ 0 & 0 & r_{41} \end{pmatrix}$$

that is only the r_{41} (or $r_{23,1} = r_{YZ,X}$) $= r_{52} = r_{63}$ does not vanish by symmetry. This implies in turn that in a Senarmont type of experimental set-up [9], only a longitudinal

modulation can be measured, corresponding to the following equation for the indicatrix:

$$\frac{Y^2}{n_0^2} + \frac{Z^2}{n_0^2} + 2r_{YZ,X}E_X YZ = 1 \tag{4}$$

for the laser light propagating along the X direction; n_0 is the refractive index and E_X the component along X of the modulating electric field.

Reduction of the above indicatrix equation to its principal axes gives two different refractive indices:

$$n_{2X} = \frac{1}{\sqrt{1/n_0^2 + r_{YZ,X}E_X}}$$
$$n_{3X} = \frac{1}{\sqrt{1/n_0^2 - r_{YZ,X}E_X}} \tag{5}$$

thus exhibiting an electric field induced birefringence given by

$$\Delta n_{23X} = n_{2X} - n_{3X} \cong n_0^3 r_{YZ,X}E_X. \tag{6}$$

All the measurements performed on the same sample used for Raman scattering gave a response drowned in the instrumental noise, in spite of the very low value of the latter. It is therefore impossible to choose between the two possibilities: either too weak an $r_{YZ,X}$ Pockels coefficient, or a symmetry vanishing one.

Consequently, the question of the space group of CNGG is still open, in spite of the $I2_13 = T^5$ (No 199) preference due to the present infrared and Raman results and to the conclusions of [2].

Acknowledgments

The authors acknowledge Professor J J Heizmann and Mr C Laruelle for x-ray pole figures, structural and orientational data obtained on our samples. They also acknowledge Dr M Aillerie for electrooptic measurements.

References

[1] Shimamura K, Timoshechkin M, Sasaki T, Hoshikawa K and Fukuda T 1993 *J. Crystal Growth* **128** 1021
[2] Ono Y, Shimamura K, Morii Y, Fukuda T and Kajitani T 1995 *Physica* B **213/214** 420
[3] Shimamura K, Sugiama K, Uda S and Fukuda T 1995 *Japan. J. Appl. Phys.* **34** 4894
[4] Carabatos-Nédelec C, Bréhat F and Wyncke B 1991 *Infrared Phys.* **31** 611
[5] Gervais F and Arend H 1983 *Z. Phys.* B **50** 17
[6] Gervais F 1983 *Infrared and Millimeter Waves* vol 8, ed K J Button (New York: Academic)
[7] Rieder K H, Weinstein B A, Cardona M and Biltz H 1973 *Phys. Rev.* B **8** 4780
[8] Fontana M D, Metrat G, Servoin J L and Gervais F 1984 *J. Phys. C: Solid State Phys.* **16** 483
[9] Aillerie M, Fontana M D, Abdi F, Carabatos-Nédelec C, Theofanous N and Alexakis G 1989 *J. Appl. Phys.* **65** 2406